


RESEARCH ARTICLE | SEPTEMBER 01 1998

## Quantum features of Brownian motors and stochastic resonance

Peter Reimann; Peter Hänggi

 Check for updates

Chaos 8, 629–642 (1998)

<https://doi.org/10.1063/1.166345>



### AIP Advances

#### Why Publish With Us?

-  **19 DAYS**  
average time  
to 1st decision
-  **500+ VIEWS**  
per article (average)
-  **INCLUSIVE**  
scope

[Learn More](#)



# Quantum features of Brownian motors and stochastic resonance

Peter Reimann and Peter Hänggi

Universität Augsburg, Memminger Str. 6, D-86135 Augsburg, Germany

(Received 2 February 1998; accepted for publication 17 April 1998)

We investigate quantum Brownian motion sustained transport in both, adiabatically rocked ratchet systems and quantum stochastic resonance (QSR). Above a characteristic crossover temperature  $T_0$  tunneling events are rare; yet they can considerably enhance the quantum-noise-driven particle current and the amplification of signal output in comparison to their classical counterparts. Below  $T_0$  tunneling prevails, thus yielding characteristic novel quantum transport phenomena. For example, upon approaching  $T=0$  the quantum current in Brownian motors exhibits a tunneling-induced reversal, and tends to a finite limit, while the classical result approaches zero without such a change of sign. As a consequence, similar current inversions generated by quantum effects follow upon variation of the particle mass or of its friction coefficient. Likewise, in this latter regime of very low temperatures the tunneling dynamics becomes increasingly coherent, thus suppressing the semiclassically predicted QSR. Moreover, nonadiabatic driving may cause driving-induced coherences and quantized resonant transitions with no classical analog. © 1998 American Institute of Physics. [S1054-1500(98)00903-3]

**Traditional heat engines are devices to extract useful work out of thermal fluctuations by way of transferring heat between equilibrium baths at different temperatures. More realistic setups, involving also nonthermal forces, have been addressed in recent years under the label of “Brownian motors.” Given the typically tiny scales of such devices, it is just one more natural step forward to also take into account quantum mechanical effects. Another instance, where noise plays a constructive role with many astonishing finer details, is “stochastic resonance,” arising in a large class of systems when driven out of thermal equilibrium by a coherent (e.g., periodic) signal. Again, the question about quantum effects poses itself in numerous systems, and often leads to highly surprising new answers compared to a purely classical approach. We shall show here that some basic ingredients of a quantum Brownian motor are related to those of stochastic resonance, especially the consistent quantum mechanical modeling of the thermal heat baths. On the other hand, the fluctuation-driven amplification of the response that characterizes stochastic resonance is governed by a mechanism which distinctly differs from the physics ruling current in Brownian motors.**

## I. INTRODUCTION

The quest of extracting usable work from unbiased fluctuations has provoked debates ever since the early days of Brownian motion theory.<sup>1</sup> *Prima facie* speaking, periodic structures that possess an intrinsic spatial asymmetry (so termed ratchets) seem capable of generating the desired directed transport. Yet, as already argued by Smoluchowski and later by Feynman,<sup>1</sup> no *stationary* net transport is possible if only equilibrium fluctuations are at work—in perfect agreement with the second law of thermodynamics. Thus finite transport with unbiased sources can emerge only under

nonequilibrium conditions. In recent years, a great variety of such classical nonequilibrium models have been demonstrated to indeed operate,<sup>2,3</sup> entailing a lot of interesting potential applications both for biological intercellular transport processes and for technological devices that pump Brownian particles on periodic structures with period length scales extending from nano to mesoscopic and even to macroscopic size. Another phenomenon where the cooperative role of (thermal or nonthermal) fluctuations, acting on systems out of equilibrium, provides a useful tool is *stochastic resonance* (SR).<sup>4-6</sup> This term is given to a phenomenon which is manifest in nonlinear metastable systems whereby—generally feeble—input information can be amplified, and optimized, by the assistance of noise. The effect apparently requires three basic ingredients: (i) an energy activation barrier or, more generally, a type of threshold; (ii) a weak coherent input (such as a periodic signal); and (iii) a source of noise which is inherent in the system (thermal), or which adds to the coherent input (nonthermal). Given these features, the response of the system undergoes a resonancelike behavior as a function of increasing noise strength; hence the name stochastic resonance. The underlying basic mechanism seems fairly simple and robust, so that it is observed in a large variety of physical, chemical, and biological systems.

The challenge here will be to pinpoint the cooperative role of quantum fluctuations, allowing for a distinct new channel for transport, namely under-barrier (-threshold) *quantum tunneling*. We shall restrict the discussion to the technologically important class of (deterministic or noisy) rocked metastable systems. In case of a ratchet this typifies a *Brownian quantum rectifier*. In a double well potential a periodic deterministic signal force represents the archetype for quantum stochastic resonance (QSR). Both systems have been investigated in recent years in the classical limit of overdamped Brownian motion,<sup>3,5,6</sup> but only recently has the study been extended to account for quantum fluctuations.

This latter objective is by no means a trivial extension; this is due to the fact that a description for a *dissipative* quantum dynamics in the presence of external, time-dependent forcing is required: Because no consistent phenomenological quantum description of damped systems does exist, the approach necessitates a firm basis that is rooted in an *ab initio* microscopic description of a total system, consisting of the metastable subsystem of relevance coupled to a “heat-reservoir” containing the microscopic degrees of freedom that provide a friction mechanism and generate fluctuational effects.

In the following series of sections we shall address this challenge of quantum-noise-driven transport in ratchets and in rocked double well systems exhibiting SR. Mostly, though not exclusively, we restrict the discussion to weak thermal quantum noise and sufficiently large barrier heights so that a description on a semiclassical level is possible. Then both phenomena can be described within a *quantum rate description*.<sup>7</sup> The current in rocked quantum ratchets is related to the *difference* of two corresponding quantum rates for forward and backward tunneling assisted (incoherent) escape; in contrast, QSR is ruled by the total rate of decay of population—given by the *sum* of these two escape rates—and the strength of *synchronization* with the deterministic time-periodic perturbation, as measured by the frequency-dependent response function for the output signal. This also shows that the two phenomena are in fact *not* really closely related with each other. It is true that both the current response and QSR generally exhibit a bell-shaped behavior versus increasing thermal noise level, as measured by the temperature  $T$ . The corresponding maxima, however, generally occur at completely different temperature values, due to the *different enhancement mechanisms* at work.

We begin our investigation of quantum Brownian motion-driven transport in metastable, driven systems with the outline of an appropriate microscopic model for friction and thermal fluctuations.

## II. TRANSPORT IN ADIABATICALLY ROCKED QUANTUM RATCHETS

### A. Model

Our starting point is a one-dimensional quantum particle with mass  $m$  in an asymmetric, periodic “ratchet”-potential  $V(x)$  of period  $L$  in the presence of a time-dependent force field  $f(t)$  that is unbiased on average. This “bare system” is furthermore coupled via coupling strengths  $c_j$  to a model “heat bath” of infinitely many harmonic oscillators with masses  $m_j$  and frequencies  $\omega_j$  ( $\omega_j > 0$  without loss of generality) yielding the compound (system-plus-environment) Hamiltonian

$$\mathbf{H}(t) = \frac{\mathbf{p}^2}{2m} + V(\mathbf{x}) - \mathbf{x}f(t) + \mathbf{H}_B, \quad (1)$$

$$\mathbf{H}_B = \sum_{j=1}^{\infty} \frac{\mathbf{p}_j^2}{2m_j} + \frac{1}{2} m_j \omega_j^2 \left( \mathbf{x}_j - \frac{c_j \mathbf{x}}{m_j \omega_j^2} \right)^2. \quad (2)$$

Here,  $\mathbf{x}$  and  $\mathbf{p}$  are the coordinate and momentum operators of the quantum Brownian particle of interest, while  $\mathbf{x}_j$  and  $\mathbf{p}_j$  are those of the bath oscillators. As initial condition at time

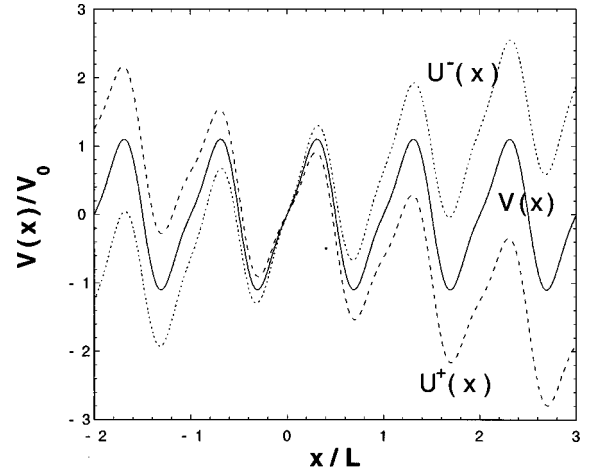


FIG. 1. Solid: ratchet potential  $V(x)$  in (5). Dashed and dotted: “tilted washboard potentials”  $U^\pm(x)$  in (7) with  $Fl=0.1V_0$ ,  $l=L/2\pi$ . Note that the extrema and the separating barriers are *different* for  $U^+(x)$  and  $U^-(x)$ , while the period  $L$  is in common.

$t=0$  we assume that the bath is at thermal equilibrium and is decoupled from the system. The infinite number of oscillators guarantees an infinite heat capacity and thus a reasonable model of a bath that keeps its initial temperature  $T$  for all later times  $t > 0$ . For the rest, it turns out that the effect of the environment on the system is completely fixed by the frequencies  $\omega_j$  and the ratios  $c_j^2/m_j$  or, equivalently, by the so-called spectral density

$$J(\omega) = \frac{\pi}{2} \sum_{j=1}^{\infty} \frac{c_j^2}{m_j \omega_j} \delta(\omega - \omega_j). \quad (3)$$

More details about this model for quantum dissipation can be found, e.g., in Refs. 7 and 8.

The observable of central interest in our above-defined ratchet dynamics is the particle current in the steady state,

$$I = \lim_{t \rightarrow \infty} \overline{\langle \dot{\mathbf{x}}(t) \rangle}_\beta, \quad (4)$$

where  $\beta = 1/k_B T$ ,  $k_B$  is Boltzmann’s constant, the subscript  $\beta$  indicates thermal averaging (quantum statistical mechanical expectation value), and the overbar indicates a time average over the (unbiased) driving force  $f(t)$ . Note that this quantity  $I$  is independent of the initial condition for the Brownian particle at time  $t=0$ .

Having specified the general model, let us now highlight some of its basic properties and introduce typical examples. The model “ratchet”-potential we will use in our numerical studies is

$$V(x) = V_0 [\sin(2\pi x/L) - \frac{1}{4} \sin(4\pi x/L)] \quad (5)$$

(see Fig. 1). Further, we will assume a so-called Ohmic bath, characterized by a continuous spectral density  $J(\omega)$  with a linear initial growth, a “cut-off” frequency  $\omega_c$ , and a single “coupling parameter”  $\eta$ :

$$J(\omega) = \eta \omega \exp\{-\omega/\omega_c\}. \quad (6)$$

The cutoff  $\omega_c$  is introduced in order to avoid unphysical ultraviolet divergences but is always chosen much larger

than any other characteristic frequency of the system and therefore typically drops out of the final results. This harmonic oscillator model for the thermal environment (1) together with the truncated Ohmic spectral density (6) has proven to provide reasonable approximations in a wide variety of real situations, even though for many complex systems, one actually does not have a clear understanding of the microscopic origin of the damping.<sup>8</sup> It should also be mentioned that, though we speak here of a particle,  $\mathbf{x}(t)$  may as well represent any other kind of relevant collective coordinate.

The force field  $f(t)$  may be either externally imposed (in experiments or technical applications) or mimic system-intrinsic collective degrees of freedom *far from thermal equilibrium* (in intracellular transport processes). This justifies that we did not include a full quantum mechanical model for this force and that we have neglected both a back-coupling of the system coordinate  $\mathbf{x}$  to  $f(t)$  as well as a possible direct interaction between the thermal environment and  $f(t)$ . For the rest, we remark that  $f(t)$  may still be either of stochastic or of deterministic nature.

For reasons of numerical efficiency only, we shall focus on a driving  $f(t)$  that can take on only the two values  $\pm F$  and is furthermore compatible with our above assumption that it is unbiased, i.e., its time average vanishes. In other words, at each instance of time, our quantum Brownian particles are exposed to either of the two ‘‘tilted washboard’’ potentials

$$U^\pm(x) = V(x) \mp Fx \tag{7}$$

(cf. Fig. 1). As a further assumption we require that  $F$  is positive but not too large, such that both potentials  $U^\pm(x)$  still display a local maximum and minimum within each period  $L$ . To fix notations, let us denote by  $x_0^\pm$  one of the local minima of  $U^\pm(x)$  and by  $x_b^\pm$  its neighboring local maximum to the right. The potential barrier which a particle at  $x = x_0^\pm$  is facing to its right is therefore  $\Delta U_r^\pm = U^\pm(x_b^\pm) - U^\pm(x_0^\pm)$  and to its left  $\Delta U_l^\pm = U^\pm(x_b^\pm - L) - U^\pm(x_0^\pm)$ . Taking into account (7) and the periodicity of  $V(x)$  it follows that

$$\Delta U_l^\pm = \Delta U_r^\pm \pm FL. \tag{8}$$

While indices  $\pm$  will often be dropped in the following, it should be emphasized that the location of the local maxima and minima, their mutual distance, as well as the corresponding potential curvatures and separating barriers are in general different for  $U^+(x)$  and  $U^-(x)$ . The only common feature is the periodicity  $L$  and the average tilt (in modulus) (see also Fig. 1).

For an arbitrary time scale of the flips of  $f(t)$  between  $\pm F$  we are still faced with an extremely difficult time-dependent quantum mechanical nonequilibrium problem. Since no way of tackling that is known to us, we henceforth restrict ourselves to very rare flips between  $\pm F$  such that transients after each flip are negligible and we can focus on the steady-state particle currents  $I^\pm$  in the two tilted washboard potentials (7). Recalling that  $f(t)$  is unbiased, i.e., on average the particle is exposed half of the time to either of potentials, the resulting net particle current (4) then immediately follows from  $I^\pm$  as

$$I = \frac{1}{2} [I^+ + I^-]. \tag{9}$$

It is instructive to notice that by way of integrating out the bath degrees of freedom in (1) one obtains<sup>7,8</sup> the following one-dimensional Heisenberg equation (generalized Langevin equation) for the position operator  $\mathbf{x}$ :

$$m\ddot{\mathbf{x}} + V'(\mathbf{x}) - f(t) = \boldsymbol{\xi}(t) - \int_0^t \hat{\eta}(t-t') \dot{\mathbf{x}}(t') dt'. \tag{10}$$

While the left-hand side can be associated to the bare system dynamics, the right-hand side accounts for the influence of the environment through the damping kernel,

$$\hat{\eta}(t) = \frac{2}{\pi} \int_0^\infty d\omega \omega^{-1} J(\omega) \cos(\omega t), \tag{11}$$

and the operator valued quantum noise,

$$\boldsymbol{\xi}(t) = \sum_{j=1}^\infty c_j \left( \frac{\mathbf{p}_j(0)}{m_j \omega_j} \sin(\omega_j t) + \left( \mathbf{x}_j(0) - \frac{c_j \mathbf{x}(0)}{m_j \omega_j^2} \right) \cos(\omega_j t) \right), \tag{12}$$

containing the initial conditions of the bath and of the particle’s position. Exploiting the assumed thermal distribution of the bath  $\mathbf{H}_B$  at  $t=0$  one sees<sup>8</sup> that  $\boldsymbol{\xi}(t)$  becomes a stationary Gaussian noise with mean value zero. Moreover, one recovers the usual connection [via  $J(\omega)$ ] between the random and the frictional effects of the bath on the right-hand side of (10) in the form of the fluctuation–dissipation relation

$$\langle \boldsymbol{\xi}(t) \boldsymbol{\xi}(t+\tau) \rangle_\beta = \frac{\hbar}{\pi} \int_0^\infty d\omega J(\omega) \times \left[ \coth\left(\frac{\hbar \omega \beta}{2}\right) \cos(\omega \tau) - i \sin(\omega \tau) \right]. \tag{13}$$

The special role of an Ohmic heat bath (6) becomes now apparent by observing that the damping kernel (11) approaches

$$\hat{\eta}(t) = 2\eta \delta(t) \tag{14}$$

when the cutoff  $\omega_c$  goes to infinity. The last term in (10) thus boils down to the memoryless Stokes friction  $\eta \dot{\mathbf{x}}(t)$ . In other words,  $\eta$  in (6) has the meaning of a damping coefficient due to viscous friction.

With the time between flips of  $f(t)$  and the cutoff  $\omega_c$  in (6) becoming asymptotically large, we are essentially left with six model parameters, namely the particle mass  $m$ , the ‘‘potential parameters’’  $V_0$ ,  $L$ , and  $F$  in (5) and (7), and finally the coupling  $\eta$  in (6) and the temperature  $T$ , characterizing the thermal environment. The necessary restrictions regarding their admitted range are most naturally discussed in the classical limit.

### B. Classical limit

The classical limit means roughly speaking to let  $\hbar$  go to zero. More precisely it is expressed by the condition that  $\hbar \beta$

becomes negligibly small in comparison with any other characteristic time scale of the system. In this limit one can infer from (13) and (6) (with  $\omega_c \rightarrow \infty$ ) that

$$\langle \xi(t) \xi(t + \tau) \rangle_\beta = 2\eta k_B T \delta(\tau). \tag{15}$$

Furthermore, quantum fluctuations will vanish, so that  $q$ -numbers go over into  $c$ -numbers in (10). Together with (14) this yields the familiar classical stochastic differential equation for the real-valued coordinate  $x(t)$ ,

$$m\ddot{x} + V'(x) - f(t) = 2\eta k_B T \zeta(t) - \eta \dot{x}, \tag{16}$$

with a  $\delta$ -correlated Gaussian noise  $\zeta(t)$ .<sup>7</sup>

We now make the assumption that the remaining model parameters  $m$ ,  $V_0$ ,  $L$ ,  $F$ , and  $\eta$  are such that a classical particle which starts at rest close to any local maximum of  $U^\pm(x)$  will *deterministically* slide down the corresponding slope but will not be able to subsequently surmount any further potential barrier and so is bound to end in the next local minimum. Differently speaking, a moderate-to-strong friction dynamics is considered and deterministically ‘‘running solutions’’ are excluded. We further assume weak thermal noise, that is, any potential barrier is much larger than the thermal energy:

$$\Delta U_{r,l}^\pm \gg k_B T. \tag{17}$$

Then, the thermally induced escape rate over each such barrier is well approximated by the classical Kramers rate in the spatial diffusion limit<sup>7</sup>

$$k_{cl} = \frac{\mu \sqrt{U_0''}}{2\pi \sqrt{|U_b''|}} \exp\{-\beta \Delta U\}, \tag{18}$$

$$\mu = \frac{\sqrt{\eta^2 + 4m|U_b''|} - \eta}{2m}, \tag{19}$$

where for the sake of better readability, indices  $r$ ,  $l$ , and  $\pm$  have been dropped, and where  $U_0''$  and  $U_b''$  represent the potential curvatures (second derivatives) at the extrema  $x_0^\pm$  and  $x_b^\pm$ , respectively. In the fixed potential  $U^+(x)$  one thus has a rate  $k_{cl,r}^+$  of the form (18) describing thermal hopping to the right, i.e., over  $\Delta U_r^+$ , and a second rate  $k_{cl,l}^+ = k_{cl,r}^+ e^{-\beta FL}$  [where we exploited (8)] for hopping to the left over  $\Delta U_l^+$ , inducing a net particle current  $I_{cl}^+ = L(k_{cl,r}^+ - k_{cl,l}^+)$ . The latter is positive in view of  $I_{cl}^+ = Lk_{cl,r}^+(1 - e^{-\beta FL})$  and since we assumed that  $F > 0$ . Analogously, in the quenched potential  $U^-(x)$  one finds the negative current  $I_{cl}^- = -Lk_{cl,l}^-(1 - e^{-\beta FL})$ . The resulting average classical current (9) can thus be rewritten as

$$I_{cl} = \frac{L}{2} (1 - e^{-\beta FL}) (k_{cl,r}^+ - k_{cl,l}^-). \tag{20}$$

### C. Semiclassical theory

Next we return to the dissipative quantum dynamics (10) but restrict ourselves to the so-called semiclassical regime. Very roughly speaking, this means that in the absence of the heat bath  $\mathbf{H}_B$  there exists a large number of (quasi-) bound states in each metastable minimum of  $U^\pm(x)$ , i.e.,  $\hbar \omega_0^\pm \ll \Delta U_{r,l}^\pm$ , where

$$\omega_0^\pm = [U_0''^\pm/m]^{1/2} \tag{21}$$

are the respective ground state frequencies. By a refined argument, this condition can still be made weaker by a factor  $2\pi$  and, after also properly taking into account the effects of the heat bath, is found to take on the final form<sup>9,10</sup>

$$\hbar \mu^\pm \ll 2\pi \Delta U_{r,l}^\pm \tag{22}$$

with  $\mu^\pm$  like in (19). Within the so-defined semiclassical realm, speaking of a particle with a reasonably well-defined position *and* momentum still makes sense except during the now possible tunneling processes, which are manifestly far from classical, but can occur with a small probability semiclassically. Moreover, tunneling between potential wells in either of the tilted washboard potentials (8) is incoherent and well described in terms of rates. As a consequence, the reasoning at the end of the preceding Sec. II B can be taken over essentially unchanged apart from the classical rates  $k_{cl}$  appearing in the current (20) which have to be replaced by their quantum mechanical counterparts  $k_{qm}$  to obtain

$$I_{qm} = \frac{L}{2} (1 - e^{-\beta FL}) (k_{qm,r}^+ - k_{qm,l}^-). \tag{23}$$

Qualitatively, each such rate  $k_{qm}$  in (23) is governed by a competitive interplay between the very rare thermal activation up to a certain ‘‘energy level’’ and the also very unlikely tunneling from there on ‘‘through’’ the remaining part of the potential barrier. Quantitatively, a sophisticated line of reasoning has been elaborated during recent years<sup>7</sup> which we will only briefly sketch in the following. Starting with the Hamiltonian system-plus-reservoir model (1) and adopting Langer’s ‘‘imaginary free energy method’’<sup>7,10</sup> or, equivalently, Miller’s ‘‘multidimensional quantum transition state theory,’’<sup>7</sup> it is possible to express the escape rate  $k_{qm}$  in terms of functional path integrals. After integration over the harmonic bath modes and a steepest descent approximation [justified by (22)] in the remaining single-variable path integral, one obtains the following form for the semiclassical approximation of the rate

$$k_{qm} = A \exp\{-S_B/\hbar\}. \tag{24}$$

Here, the exponentially dominating contribution  $S_B$  is defined via the nonlocal action

$$S[q] = \int_0^{\hbar\beta} d\tau \left[ \frac{m\dot{q}^2}{2} + U(q) + \frac{\eta}{4\pi} \int_{-\infty}^{\infty} d\tau' \left( \frac{q - q'}{\tau - \tau'} \right)^2 \right] \tag{25}$$

with the abbreviations  $q = q(\tau)$  and  $q' = q(\tau')$ , and where we exploited the assumed Ohmic spectral density (6) with  $\omega_c \rightarrow \infty$  (generalizations are immediate, see Refs. 7 and 10). Like previously in (18) we again omitted here indices  $r$ ,  $l$ , and  $\pm$  for the sake of better readability. This action (25) has now to be extremized with respect to  $q(\tau)$  under the constraints that  $q(\tau + \hbar\beta) = q(\tau)$  for all  $\tau$ , and that there exists at least one  $\tau$  with  $q(\tau) = x_b$ . A trivial such extremizing  $q(\tau)$  is always  $q(\tau) \equiv x_b$ . Among this and the possibly existing further extrema one has to select the one that minimizes  $S[q]$ , the so-called ‘‘bounce solution’’  $q_B(\tau)$ , to finally obtain the exponentially leading contribution in (24) as

$$S_B := S[q_B] - \hbar \beta U(x_0). \tag{26}$$

Since this bounce  $q_B(\tau)$  is in fact nothing else than the dominating path in the above-mentioned steepest descent approximation of the path integral, it is obvious that the preexponential factor  $A$  in (24) accounts for the fluctuations about this dominating path, i.e., contributions to the path integral from an entire small vicinity of  $q_B(\tau)$ . The most convenient way of rewriting this prefactor  $A$  depends on the considered temperature, as discussed next.

Closer inspection shows<sup>7,10</sup> that there exists a crossover temperature

$$T_0 = \mu \hbar / 2\pi k_B \tag{27}$$

above which  $q_B(\tau) \equiv x_b$  is the only admissible extremum in (25), and therefore  $S_B / \hbar = \beta \Delta U$  according to (26). In view of (24) and (18) tunneling thus does not affect the exponentially leading part of the rate in this regime  $T \geq T_0$ . Moreover, a closed analytical expression for the prefactor  $A$  is available,<sup>7,10,11</sup> yielding for the quantum rate the result

$$k_{\text{qm}} = k_{\text{cl}} (\lambda_1^0 / \Lambda_1^b) \prod_{n=2}^{\infty} (\lambda_n^0 / \lambda_n^b). \tag{28}$$

Here, we introduced the notations

$$\lambda_n^{0,b} = m \nu_n^2 + \eta \nu_n + U''_{0,b}, \tag{29}$$

$$\nu_n = 2\pi n / \hbar \beta, \tag{30}$$

$$\Lambda_1^b = \sqrt{\mathcal{L} / \pi \beta} e^{-\beta[\lambda_1^b]^2 / \mathcal{L}} / \text{erfc}(\lambda_1^b \sqrt{\beta / \mathcal{L}}), \tag{31}$$

$$\mathcal{L} = \frac{[U''_b]^2}{|U''_b|} \frac{4m\mu^2 + |U''_b|}{2m\mu^2 + |U''_b|} + \frac{d^4 U(x_b)}{dx^4}, \tag{32}$$

where the complementary error function is given by  $\text{erfc}(z) = 2\pi^{-1/2} \int_z^{\infty} e^{-y^2} dy$  and where  $\mathcal{L} > 0$  in (32) has been tacitly assumed. It is not difficult to verify that the  $\lambda_n^b$  are the eigenvalues of the action (25) when linearized about the trivial extremizing path  $q_B(\tau) \equiv x_b$  and similarly for the  $\lambda_n^0$  and  $q(\tau) \equiv x_0$ . Close to  $T_0$  one has  $\lambda_1^b \approx 0$ , calling for special care in the steepest descent evaluation of  $A$  in (24). Accordingly, the quantity  $\Lambda_1^b$  in (31) has been obtained by properly including also next to leading order contributions in that evaluation of  $A$ . On the other hand, outside this vicinity of  $T_0$ , that is, when  $\lambda_1^b \sqrt{\beta / \mathcal{L}} \gg 1$ , one has  $\Lambda_1^b \rightarrow \lambda_1^b$  since  $\text{erfc}(z) \rightarrow \exp(-z^2) / \sqrt{\pi z}$  for  $z \rightarrow \infty$ . Now, one readily observes that  $k_{\text{qm}} \geq k_{\text{cl}}$  for all admitted  $T \geq T_0$ . Finally, when  $T \gg T_0$ , or equivalently,  $\hbar \rightarrow 0$ , all the factors multiplying  $k_{\text{cl}}$  on the right-hand side of (28) tend to unity, and thus  $k_{\text{qm}}$  smoothly approaches the classical Kramers rate (18), as it should be.

Note that the two rates in the current (23) bring along two different crossover temperatures  $T_0^+$  and  $T_0^-$  since  $|U''_b|$  in (19) and thus  $\mu$  in (27) are typically different for  $U^{\pm}(x)$ . One can now rewrite the semiclassical condition (22) in terms of those crossover temperatures as

$$k_B T_0^{\pm} \ll \Delta U_{r,l}^{\pm}. \tag{33}$$

It is reassuring to observe that in fact the semiclassical condition (22) is nothing else than the classical weak noise condition for the validity of the Kramers rate (17) at crossover  $T = T_0$ .

Turning to subcritical temperatures  $T < T_0$ , analytical progress is possible only in a few special cases.<sup>7</sup> The simplest of them is the limit  $\eta \rightarrow 0$ ,  $T \rightarrow 0$  (no heat bath), resulting in the familiar Gamow formula for the exponentially leading action (25) for tunneling decay

$$S_B \rightarrow S_G = 2 \left| \int_{x_0}^{x_1} dq \sqrt{2m[U(q) - U(x_0)]} \right|, \tag{34}$$

where  $x_1$  denotes the first point beyond the potential barrier with the property  $U(x_1) = U(x_0)$ . (The absolute value is needed since  $x_1 < x_0$  for the escapes to the left, i.e., across  $\Delta U_l^{\pm}$ .) The corresponding expression for the prefactor  $A$  is obtained as<sup>12</sup>

$$A \rightarrow A_G = \sqrt{\frac{m\omega_0^3}{\pi\hbar}} \lim_{x \rightarrow x_0} |x - x_0| \times \exp \left\{ \left| \int_x^{x_1} dq \sqrt{\frac{U''(x_0)/2}{U(q) - U(x_0)}} \right| \right\}. \tag{35}$$

In more general cases we have to resort to a numerical evaluation of the semiclassical rate.

#### D. Numerical solution below crossover

Though our numerical method to evaluate the semiclassical rate (24) in the subcrossover regime  $T < T_0$  appears to be quite natural and straightforward, we remark that prior to our work<sup>13</sup> only two comparable numerical studies have been available,<sup>10,14</sup> both focusing on a cubic potential  $U(x)$ , and exploiting heavily its special properties.

Our starting point to tackle the extremization of the action functional in (25) is a truncated Fourier series ansatz for the bounce  $q_B(\tau)$  of the form

$$q_B(\tau) = \sum_{n=0}^N c_n \cos(\nu_n \tau) + s_n \sin(\nu_n \tau) \tag{36}$$

with the Matsubara frequencies  $\nu_n$  from (30). This ansatz is suggested by the required periodicity  $q_B(\tau + \hbar \beta) = q_B(\tau)$ . Note that with  $q_B(\tau)$  also  $q_B(\tau + \Delta \tau)$  will be an equivalent solution of the extremization problem for any  $\Delta \tau$ . A natural way to get rid of this numerically quite annoying ambiguity is by setting *a priori*  $s_N = 0$  in (36). Similarly, one can set  $s_0 = 0$  for trivial reasons. Introducing now the trial function ansatz (36) into the extremization problem (25) leads—by way of requiring stationarity with respect to the remaining  $2N$  Fourier coefficients  $c_n$  and  $s_n$ —to a set of  $2N$  coupled nonlinear equations. Since multiple solutions are expected in general, this set of equations requires a rather careful numerical exploration. We also remark that the final relevant solution  $q_B(\tau)$  is by construction an extremum of the action functional (25) but can be shown to be a “true saddle point,” i.e., neither a maximum nor a minimum, so that a

direct numerical minimization/maximization of (25) is not possible. As a surprising numerical by-product we also verified in all studied cases that

$$s_n = 0 \quad \text{for all } n. \quad (37)$$

In other words, possibly after a preceding shift of the time origin, the symmetry  $q_B(-\tau) = q_B(\tau)$  is always respected. This symmetry has sometimes been tacitly assumed in the literature,<sup>10</sup> but to the best of our knowledge a general proof is still missing.

Once  $q_B(\tau)$  is determined, the action follows with (25) and the prefactor  $A$  can be obtained as<sup>7,10,11</sup>

$$A = \left| \frac{\int_0^{\hbar\beta} [\dot{q}_B(\tau)]^2 d\tau \prod \lambda_n^0}{2\pi\hbar \prod' \lambda_n^B} \right|^{1/2}, \quad (38)$$

with  $n$  running from  $-\infty$  to  $\infty$  in the products  $\Pi$ . Similarly as in (28), the  $\lambda_n^B$  here are the eigenvalues of the action (25) when linearized about  $q_B(\tau)$ . One of them is negative, reflecting the above-mentioned saddle point nature of the extremizing path  $q_B(\tau)$ , and a further one is zero, related to the fact that with  $q_B(\tau)$  also  $q_B(\tau + \Delta\tau)$  is an equally admissible extremizing path in (25) for any  $\Delta\tau$  (i.e., a Goldstone mode is present). They are usually denoted by  $\lambda_0^B$  and  $\lambda_1^B$  and are clearly the continuations of  $\lambda_0^b$  and  $\lambda_1^b$  from (28) into the deep subcritical temperature regime. The zero eigenvalue has to be omitted in (38) as indicated by the primed product; it becomes, very roughly speaking, substituted by the integral in the numerator.

By including sufficiently many Fourier coefficients in (36) and sufficiently many eigenvalues  $\lambda_n^B$  in (38) the uncertainty margin of our numerical rates is at most a few percent for arbitrary  $T \geq 0.1T_0$ . In particular, we reproduced the numerical results for a cubic metastable potential given in Ref. 10 to all digits. For completeness only, we may add that for  $T < 0.1T_0$  reliable extrapolations could be readily obtained by exploiting the known asymptotical analytic results<sup>7,10</sup> that  $S_B(T \rightarrow 0)$  remains finite,  $S_B(0) - S_B(T) \sim T^2$  for small  $T$ , and  $A(T)$  can usually be approximated quite accurately by its finite asymptotic limit  $A(T=0)$ . To cover this temperature regime will, however, not be of central importance for our ratchet problem under study.

It is well known<sup>10</sup> that the simple steepest descent approximation underlying (38) becomes invalid for temperatures  $T$  very close to crossover  $T_0$  such that  $\lambda_1^b \sqrt{\beta/\mathcal{L}}$  is of the order  $-1$  or larger [cf. (29)–(32)]. There, one rather has to match this approximation with the more sophisticated one (28) [cf. the discussion below (32)]. In fact it can be shown<sup>7,10</sup> that the validity of (28) actually extends even somewhat into the subcrossover regime as far as corrections of order  $1 - T/T_0$  in the prefactor  $A$  and of order  $(1 - T/T_0)^3$  in the action  $S_B$  in comparison to the full expression (24) are considered as negligible. However, as it turns out, this approximation is still too inaccurate for our purposes in the sense that simply matching it with the numerics at the first instance below  $T_0$  where they agree leads to obviously inadequate results.

## E. Results

In this section we shall discuss a few representative examples for the behavior of the particle current  $I$  in our quantum ratchet model. We recall that the classical prediction follows immediately from (20) and (18), while the semiclassical current (23) requires a more involved numerical evaluation of two quantum rates along the lined described in the above Sec. II D. As already mentioned, this gives rise to the two crossover temperatures  $T_0^+$  and  $T_0^-$ , and it is useful to introduce at this point the definitions

$$T_0^{\max} = \max \{T_0^+, T_0^-\}, \quad (39)$$

$$T_0^{\min} = \min \{T_0^+, T_0^-\}. \quad (40)$$

Similarly, we denote the smaller of the two potential barriers entering through (18) and (28) into the expressions for the current (20) and (23), respectively, by

$$\Delta U^{\min} = \min \{\Delta U_r^+, \Delta U_l^-\}. \quad (41)$$

Note that  $\Delta U^{\min}$  is, according to (8), in fact the smallest of all four potential barriers arising in  $U^\pm(x)$ .

We first address the behavior of the particle current  $I$  as a function of temperature  $T$  [measured in units of  $T_0^{\max}$  from (39)]. To completely fix the model, we still have to specify the five parameters  $m$ ,  $\eta$ ,  $V_0$ ,  $F$ , and

$$l := L/2\pi. \quad (42)$$

We do this by prescribing five dimensionless numbers as follows: First, we fix the three ‘‘potential parameters’’  $V_0$ ,  $F$ , and  $l$  through

$$Fl/V_0 = 0.1, \quad (43)$$

$$\Delta U^{\min}/V_0 \approx 1.819, \quad (44)$$

$$|U_+''|l^2/V_0 \approx 1.672. \quad (45)$$

The corresponding bare potential  $V(x)$  from (5) together with the two tilted washboard potentials from (7) are depicted in Fig. 1. Next we choose

$$\eta/m\omega_0^* = 1, \quad (46)$$

where

$$\omega_0^* = [V_0/l^2m]^{1/2}, \quad (47)$$

corresponding to a moderate damping as compared to inertia effects. To see this, we note that  $\omega_0^*$  approximates rather well the true ground state frequencies (21) in both potentials  $U^\pm(x)$ . Namely,  $\omega_0^+ \approx 1.239\omega_0^*$ , and  $\omega_0^- \approx 1.294\omega_0^*$ . In particular, (46) rules out the occurrence of ‘‘deterministically running classical solutions’’ both in  $U^+(x)$  and  $U^-(x)$  (cf. Sec. II B). Our last dimensionless number is

$$\frac{\Delta U^{\min}}{k_B T_0^{\max}} = 10. \quad (48)$$

In this way, the weak noise condition (17) is safely fulfilled at least up to  $T = 2T_0^{\max}$  and at the same time the semiclassical condition (22) rewritten in the form (33) is also satisfied.

The classical prediction for the current from (20) and (18) approaches a straight line for small  $T$  in the Arrhenius

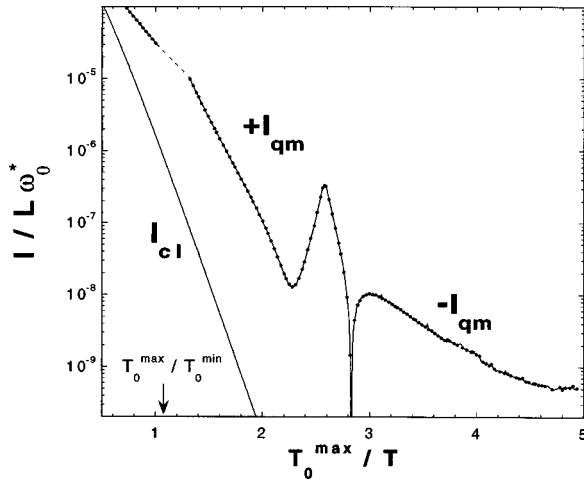


FIG. 2. The classical steady state current  $I_{cl}$  and its quantum mechanical counterpart  $I_{qm}$  for the ratchet potential from Fig. 1 in dimensionless units  $I/L\omega_0^*$ . Note that in the present Arrhenius plot (logarithmic ordinate) the observed behavior of the quantum current near  $T_0^{\max}/T=2.8$  is not the signature of a divergence but rather of a change of sign. Further worth mentioning features are the nonmonotonicity of  $I_{qm}$  and that apparently  $I_{qm}$  tends towards a finite limit when  $T\rightarrow 0$ . The exact parameters values are given through (43)–(46), and (48). For more details see main text.

plot Fig. 2. Its sign is governed by that of  $\Delta U_l^- - \Delta U_r^+$  and is thus always positive for our example potential (“forward ratchet,” cf. Fig. 1). Furthermore, Fig. 2 depicts the quantum current above crossover ( $T_0^{\max} \leq T \leq 2T_0^{\max}$ ) according to (23) and (28). In a close vicinity of either of the crossover temperatures  $T_0^\pm$ , an increased uncertainty of the semiclassical rate theory arises, as discussed at the end of Sec. II C. This gap in our data between roughly  $T_0^{\max}$  and  $T_0^{\min}$  is bridged by the dashes in Fig. 2. For even smaller  $T < T_0^{\min}$  the results shown in Fig. 2 have been obtained by the numerical procedure from Sec. II D. The slight roughness in the curve at very low  $T$  is due to numerical inaccuracies [they are not visible in the individual rates but only in the much more sensitive *difference* of rates entering into (23)].

Our first observation is that even above  $T_0^{\max}$ , quantum effects may *enhance* the classical directed transport by more than a *decade*. They become negligible only beyond several  $T_0^{\max}$ . In other words, significant quantum corrections of the classically predicted particle current set in already well above the crossover temperature  $T_0$ , where tunneling processes are still rare. (They can be associated to quantum effects other than genuine tunneling “through” a potential barrier.<sup>8</sup>) With decreasing temperature,  $T < T_0^{\min}$ , quantum transport is even much more enhanced in comparison with the classical results. A further remarkable feature caused by the intriguing interplay between thermal noise and quantum tunneling is the *inversion* of the quantum current direction at very low temperatures. In a classical description, such a reversal for adiabatically slow driving is ruled out (see Ref. 15). Finally,  $I_{qm}$  approaches a finite (negative) limit when  $T\rightarrow 0$ , implying a finite (*positive*) stopping force<sup>3</sup> also at  $T=0$ . In contrast, the classical prediction  $I_{cl}$  remains positive but becomes arbitrarily small with decreasing  $T$ . A curious detail in Fig. 2 is the nonmonotonicity of  $I_{qm}$  around  $T_0^{\max}/T \approx 2.5$ . It is caused by a similar resonancelike  $T$  de-

pendence in one of the underlying quantum rates that is further enhanced due to the fact that a *difference* of such rates governs the current (23). A better understanding of this issue is the subject of ongoing work.

We also studied other parameter values than those used in Fig. 2 as well as somewhat modified potentials (5). As an example we refer to the results presented in Ref. 13. Basically, always the same qualitative behavior is observed, except that the nonmonotonic temperature dependence disappears for sufficiently large  $\Delta U^{\min}/k_B T_0^{\max}$  values. Thus all the above-described novel features appear to be typical for a large class of quantum ratchet systems.

To explain qualitatively the current reversal, we recall that in the limit  $T\rightarrow 0$  and  $\eta\rightarrow 0$  the exponentially leading contribution  $S_B$  in the semiclassical rate (24) is given by the Gamow factor  $S_G$  from (34). Strictly speaking, by letting  $\eta\rightarrow 0$  we of course violate the assumption that deterministically running solutions should be ruled out. However, it is plausible that small but finite  $\eta$  will exist for which the following qualitative arguments can be adapted self-consistently. In that spirit, we now proceed to conclude from (23) that the sign of the quantum current will be governed by that of the difference  $S_{G,l}^- - S_{G,r}^+$  between the Gamow factors (34) belonging to the two rates in (23). The fact that this difference is negative cannot definitely be read off by eye directly from Fig. 1 since it is rather small, but is readily verified numerically. In other words, for very small  $T$  indeed a negative current is predicted. On the other hand, for large  $T$  we are approaching the classical limit,  $I_{qm}\rightarrow I_{cl}$ , and the positive sign of  $I_{cl}$  (as discussed above) carries over to  $I_{qm}$ . A change of sign in  $I_{qm}$  at some intermediate temperature is thus a necessary consequence. For more general  $\eta$  and  $T$ , quantum tunneling and thermal effects are well known to conspire in a very complicated and often counter-intuitive way so that simple explanations usually cannot be given.

The occurrence of current reversals in ratchet models when certain control parameters are varied has been a major issue of several investigations. It has, however, not always been sufficiently appreciated that typically such a change of sign is immediately carried over to the dependence of the current on many other model parameters.<sup>16</sup> We exemplify this observation by choosing in Fig. 2 a temperature  $T = T_0^{\max}/2.8$  very close to the current-inversion point, but now keep  $T$  fixed and vary some other parameter instead. Results with the mass  $m$  and the friction coefficient  $\eta$  as such control parameters are given in Figs. 3 and 4, respectively. Since reversals with respect to  $T$  are apparently rather typical, the same may be expected with respect to  $m$  and  $\eta$  as well. Such a sensitive dependence of the current direction on basic properties of the Brownian particles is of considerable interest both with respect to possible new particle-separation methods as well as for modeling of biological transport processes.<sup>2,3</sup>

### III. QUANTUM STOCHASTIC RESONANCE

#### A. General framework

We now turn to the constructive role of quantum fluctuations for the phenomenon of *quantum stochastic reso-*



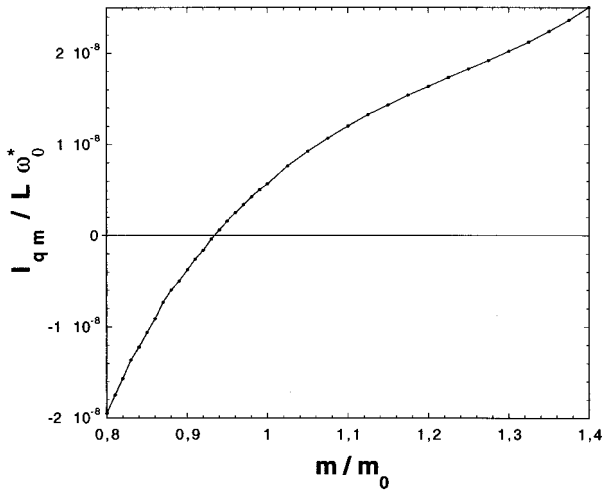


FIG. 3. The steady-state quantum current in dimensionless units  $I_{qm}/L\omega_0^*$  versus particle mass. This plot was obtained by first taking in Fig. 2  $T = T_0^{\max}/2.8$  and with  $m_0$  defined as the corresponding value of the particle mass [ $m_0 = \eta/\omega_0^*$  according to (46)]. This temperature was then kept fixed while the mass  $m$  was varied.

nance (QSR). Quantum effects enter the dynamics of a nonlinear bistable system whenever its size is no longer of macroscopic extent and/or when characteristic classical energy scales, for example the thermal energy  $k_B T$ , become comparable with typical quantum mechanical energies. The thermal de Broglie wavelength then is no longer much smaller than all other characteristic length scales of the system. This regime characterizes what we shall term the “deep quantum regime.” With the smallest characteristic energy scale given in a bistable quantum system by the level splitting  $\Delta$  of the lowest doublet, the corresponding temperatures are generally very low. For macroscopic quantum systems such as Josephson junctions or superconducting quantum interference devices (SQUIDs) they are in the milli-Kelvin region, but can reach values around room temperatures for systems of molecular or atomic size. Quantum effects, how-

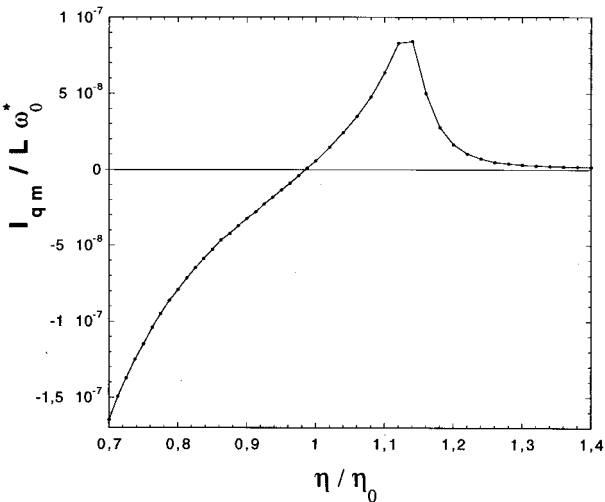


FIG. 4. The same as in Fig. 3 but with the friction coefficient  $\eta$  used as a control parameter [ $\eta_0 = m\omega_0^*$  according to (46)].

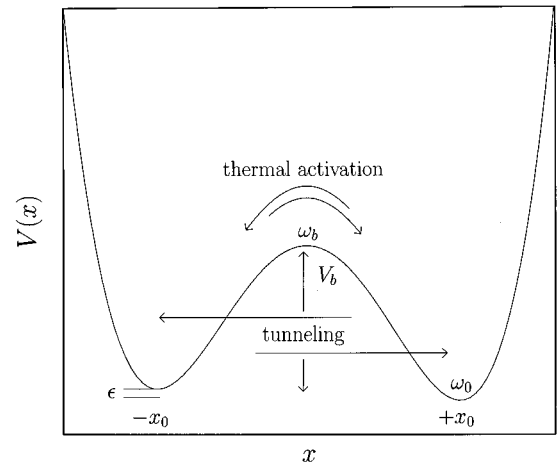


FIG. 5. Interplay of thermal activation and quantum fluctuations for quantum stochastic resonance in an asymmetric bistable potential with asymmetry parameter  $\epsilon$ .

ever, manifest themselves, as demonstrated in the previous section, already at much higher temperatures, namely around and even well above the cross-over temperature  $T_0$ . Even up to several  $T_0$ , the classical thermally activated transition over a barrier is already notably affected by finite quantum reflection and quantum transmission probabilities.

Let us first investigate this semiclassical regime of SR<sup>17</sup> near and above the crossover temperature where quantum effects start to appreciably modify the classical SR dynamics. Like in (1) and (2), we consider again a quantum particle of mass  $m$  moving in a generally asymmetric bistable potential  $V(x)$  (see Fig. 5), which is bilinearly coupled to a heat bath of harmonic degrees of freedom, generating the quantum friction mechanism according to an Ohmic spectral density (6). Simultaneously, the system is subject to a time-dependent periodic force

$$f(t) = -A \cos \Omega t. \tag{49}$$

The bistable potential  $V(x)$  is characterized by an asymmetry parameter  $\epsilon \geq 0$  with the dimension of an energy such that for  $\epsilon = 0$  the potential is symmetric,  $V(-x) = V(x)$ . For an arbitrary but fixed  $\epsilon$ , the two metastable minima are located at  $\pm x_0$ , the maximum in between is denoted by  $x = x_b$ , yielding a maximal tunneling length  $2x_0$ , and the respective barrier heights to be surmounted by a particle located at  $\pm x_0$  can be written without loss of generality in the form

$$E_{\pm} = V_b \mp \epsilon/2. \tag{50}$$

The potential curvatures at the barrier and the wells are again conveniently characterized by the respective “barrier-” and “well-frequencies:”

$$\omega_b := [ |V''(x_b)|/m ]^{1/2}, \quad \omega_0 := [ |V''(\pm x_0)|/m ]^{1/2}. \tag{51}$$

Note that for not too large  $\epsilon$ , the implicitly assumed symmetry with respect to the potential curvatures at the two wells [ $V''(-x_0) = V''(x_0)$ ] is not a serious loss of generality, given the exact symmetry  $V(-x) = V(x)$  for  $\epsilon = 0$ . We also remark that the parameters  $x_{0,b}$ ,  $\omega_{0,b}$ , and  $V_b$  may still vary upon changing  $\epsilon$  and that further details of  $V(x)$  will usually not

play any role later on. Next, we recall that the exact, dissipative quantum dynamics is again governed by the quantum Langevin equation in (10) with the corresponding Ohmic friction kernel (14) and with operator-valued quantum fluctuations  $\xi(t)$ , satisfying (13). Finally, much like in Sec. II B, the concept of metastability holds true only when the barrier is large enough so that the forward rate of escape  $k^+$  as well as the backward rate  $k^-$  are *small* compared with all the other characteristic inverse time scales of the system dynamics. In particular, because the angular frequency  $\omega_0$  describes the time scale for relaxation within a metastable well, the activation energies  $E_{\pm}$  must be sufficiently large compared to the thermal energy  $k_B T$  to ensure that the condition  $\omega_0 \gg k^{\pm}$  is fulfilled.<sup>7</sup> In other words, we require that

$$V_b - \epsilon/2 \gg k_B T. \quad (52)$$

The basic quantity of interest for SR is the time-dependent quantum statistical mechanical expectation value of the particle's position, averaged over the reduced density operator  $\rho_{red}(t)$ , becoming periodic at asymptotic times  $t$  (see below), i.e.,

$$P(t) := \langle \mathbf{x}(t) \rangle. \quad (53)$$

It constitutes the output of the system when the external time-periodic force  $f(t)$  (49) is acting. Besides  $P(t)$ , the averaged power spectrum  $\bar{S}(\omega)$ ,

$$\bar{S}(\omega) := \int_{-\infty}^{+\infty} d\tau e^{i\omega\tau} \bar{C}(\tau) = S_N(\omega) + S^{(as)}(\omega), \quad (54)$$

defined as the Fourier transform of the time-averaged quantum correlation function  $\bar{C}(\tau)$

$$\bar{C}(\tau) := \frac{\Omega}{2\pi} \int_0^{2\pi/\Omega} dt \frac{1}{2} \langle \mathbf{x}(t+\tau)\mathbf{x}(t) + \mathbf{x}(t)\mathbf{x}(t+\tau) \rangle, \quad (55)$$

is a further fundamental quantity to investigate SR.<sup>5,6</sup> It should be noted that, due to the explicit time dependence of the perturbation (49), the correlation function  $\langle \mathbf{x}(t+\tau)\mathbf{x}(t) + \mathbf{x}(t)\mathbf{x}(t+\tau) \rangle$  depends separately on the time arguments  $t$  and  $\tau$ . This explicit dependence on  $t$ , however, has been omitted since it will indeed drop out in the long time limit  $t \rightarrow \infty$  considered below,<sup>18</sup> thanks to the integration over a driving period in (55). As anticipated on the right-hand side of (54), for a time-periodic perturbation, the power spectrum results in the sum of two contributions, where  $S_N(\omega)$  represents, in the *absence* of signal, the broadband ‘‘noise background,’’ possessing a Lorentzian hump at  $\omega=0$ . We shall denote this contribution by  $S_N^{(0)}(\omega)$ . In the presence of the signal,  $S_N(\omega)$  is obtained as a product of the Lorentzian hump  $S_N^{(0)}(\omega)$  and a correction factor (of order unity for weak signals) describing the modification of the signal on the broadband ‘‘background.’’<sup>18,19</sup> The ‘‘asymptotic’’ contribution  $S^{(as)}(\omega)$  is given by the sum of  $\delta$ -spikes at integer multiples  $\omega = n\Omega$  of the signal frequency, reflecting the fact that, for times  $t$  large compared to the time scale of the transient dynamics, the motion acquires the periodicity of the external perturbation. Similarly,  $P(t)$  and  $\bar{C}(\tau)$  approach for large times  $t$  an asymptotically periodic behavior of the form<sup>18,20</sup>

$$P(t) \xrightarrow{t \rightarrow \infty} P^{(as)}(t) = \sum_{m=-\infty}^{\infty} P_m(\Omega, A) e^{-im\Omega t}, \quad (56)$$

$$\bar{C}(\tau) \xrightarrow{t, \tau \rightarrow \infty} C^{(as)}(\tau) = \sum_{m=-\infty}^{\infty} |P_m(\Omega, A)|^2 e^{-im\Omega \tau}. \quad (57)$$

Thus, the amplitudes  $|P_m|$  of the harmonics of  $P(t)$  determine the weights of the  $\delta$ -spikes of the averaged spectral power density in the asymptotic state  $S^{(as)}(\omega)$  via the relation

$$S^{(as)}(\omega) = 2\pi \sum_{m=-\infty}^{\infty} |P_m(\Omega, A)|^2 \delta(\omega - m\Omega). \quad (58)$$

In other words, in the most interesting regime of asymptotically large times  $t$ , the behavior of the observables  $S^{(as)}(\omega)$  and  $\bar{C}(\tau)$  follows from that of  $P(t)$  (Wiener–Khinchine theorem). The two main quantities that have been examined in the literature on SR are the spectral amplification (or power amplitude)  $\eta_1$  in the first frequency component of  $S^{(as)}(\omega)$ ,<sup>5,6,18</sup> and the ratio  $\mathcal{R}$  of  $\eta_1$  to the power spectrum  $S_N^{(0)}(\omega)$  in the absence of a signal, evaluated at the external driving frequency  $\omega = \Omega$ , the so-called signal-to-noise ratio (SNR),<sup>5,6,19</sup> i.e.,

$$\eta_1(\Omega, A) := 4\pi |P_1(\Omega, A)|^2, \quad (59)$$

$$\mathcal{R} := 4\pi |P_1(\Omega, A)|^2 / S_N^{(0)}(\Omega).$$

By definition,  $\eta_1$  has the dimension of a length squared, while  $\mathcal{R}$  has the dimension of a frequency. Thus, to investigate the interplay between noise and the coherent driving input which yields the phenomenon of QSR, we shall consider two dimensionless quantities, namely the scaled power amplification  $\tilde{\eta}_1$  and the scaled signal-to-noise ratio  $\tilde{\mathcal{R}}$ . They read

$$\tilde{\eta}_1(\Omega, A) := \frac{\eta_1(\Omega, A)}{(Ax_0^2/V_b)^2}, \quad \tilde{\mathcal{R}} := \frac{(\mathcal{R}/\omega_b)}{(Ax_0/V_b)^2}. \quad (60)$$

Thus far, all our definitions are completely general and all relations are still exact; they describe the full *nonlinear* QSR in the whole temperature regime extending from absolute zero up to room temperatures and beyond, and they approach the limit of classical nonlinear SR smoothly. The main challenge consists in the evaluation of the (exact) asymptotic quantum expectation value  $P(t)$  in (56), from which everything else follows. Since we are not able to do this in analytical closed form, we next address this challenge within a quantum linear response theory.

### B. Linear response theory for quantum stochastic resonance

Because the main focus of SR centers around the noise-driven enhancement of the response to a *weak* coherent input, we shall develop in this section the theory for QSR based on Kubo's linear response theory, which in our case—thermal equilibrium when driving is absent—can be based on the quantum fluctuation-dissipation theorem (QFDT). This theorem relates the unperturbed ( $A=0$ ) power spec-

trum of fluctuations in thermal equilibrium  $S_N^{(0)}(\omega)$  to the linear susceptibility  $\tilde{\chi}(\omega)$  at the driving frequency  $\omega = \Omega$  according to the celebrated relationship

$$S_N^{(0)}(\Omega) = \hbar \coth(\beta\hbar\Omega/2) \text{Im} \tilde{\chi}(\Omega). \quad (61)$$

In the limit  $\hbar\beta\Omega \ll 1$  the QFDT becomes  $S_N^{(0)}(\Omega) = 2 \text{Im} \tilde{\chi}(\Omega)/\beta\Omega$ , thus correctly reproducing the classical fluctuation–dissipation theorem (see also Sec. II B).

In the linear response approximation, only the harmonics  $0, \pm 1$  of  $P^{(\text{as})}(t)$  in Eq. (56) are different from zero,  $P_0$  being just the thermal equilibrium value  $P_{\text{eq}}$  in the absence of driving, and  $P_{\pm 1} = (A/2)\tilde{\chi}(\pm\Omega)$  being related by Kubo's famous formula to the linear susceptibility  $\tilde{\chi}(\Omega)$  according to

$$\tilde{\chi}(\Omega) = \frac{i}{\hbar} \int_{-\infty}^{+\infty} d\tau e^{i\Omega\tau} \theta(\tau) \langle [q(\tau), q(0)] \rangle_{A=0}, \quad (62)$$

where  $\langle \dots \rangle_{A=0}$  indicates the quantum statistical mechanical evaluation of correlation functions in *thermal equilibrium*, that is, in the absence of driving. Further,  $i\langle [q(\tau), q(0)] \rangle_{A=0}/\hbar$  becomes in the classical case the correlation function  $-\beta\langle q(0)\dot{q}(\tau) \rangle_{A=0}$ . Finally, because the linear susceptibility is related to the power spectrum in thermal equilibrium by the fluctuation–dissipation theorem (61), the quantities from (59) can be recast into the form

$$\eta_1(\Omega, A) = \pi A^2 |\tilde{\chi}(\Omega)|^2, \quad (63)$$

$$\mathcal{R} = \pi A^2 \frac{1}{\hbar \coth(\beta\hbar\Omega/2)} \frac{|\tilde{\chi}(\Omega)|^2}{\text{Im} \tilde{\chi}(\Omega)}. \quad (64)$$

Thus, for weak external signals, the computation of the spectral amplification  $\eta_1$  or of the signal-to-noise ratio  $\mathcal{R}$  is reduced to the evaluation of a dissipative, thermal quantum equilibrium correlation function in (62). This is still a very difficult task for a full nonlinear bistable potential as depicted in Fig. 5.

### C. Tunneling corrections to stochastic resonance

We shall simplify the analysis further by restricting ourselves to the regime around the crossover temperature  $T_0$  where tunneling events and classical noise-induced hopping events are of comparable importance. At such still rather high temperatures, the dissipative equilibrium quantum dynamics is solely incoherent. In addition we shall neglect the influence of small, relaxational intrawell quantum fluctuations. In principle their role could be accounted for by approximating the fast relaxational intrawell quantum motions by the weighted quantum dissipative harmonic oscillator dynamics in the left and right wells, respectively. These latter quantum dynamics can be evaluated in principle in exact closed form for all temperatures  $T$ . However, such effects would play an essential role only for the signal-to-noise ratio at small ratios of  $T/T_0$ .<sup>6,18</sup> Because we restrict the discussion here to temperatures near and above  $T_0$ , we can safely neglect their influence. As a consequence, we can derive our results within a *two-state* description of the system dynamics, by introducing the probabilities  $n_{L,R}$  for the system to be

in the left ( $n_L$ ) or right ( $n_R$ ) well of the bistable potential. For a state-continuous system,  $n_{L,R}$  are defined in terms of the probability density  $p(x, t)$  for the particle's position as

$$n_L(t) = 1 - n_R(t) = \int_{-\infty}^{x_b} dx p(x, t). \quad (65)$$

One then finds that the relaxation of an initial nonequilibrium value in Eq. (53), i.e.,  $P(t) = x_0[n_R(t) - n_L(t)]$ , is governed by a rate equation

$$\dot{P}(t) = -\bar{\Gamma}[P(t) - P_{\text{eq}}], \quad (66)$$

with

$$\bar{\Gamma} = k_{\text{qm}}^+ + k_{\text{qm}}^- \quad (67)$$

being the *sum* of the forward and backward quantum hopping rates  $k_{\text{qm}}^+$  and  $k_{\text{qm}}^-$ , respectively, and where  $P_{\text{eq}} := x_0(k_{\text{qm}}^+ - k_{\text{qm}}^-)/\bar{\Gamma}$  as a consequence of the detailed balance condition at equilibrium.<sup>7</sup> Information about the detailed form of the potential is *still* contained in the averaged rate  $\bar{\Gamma}$ . In the deep quantum regime  $T \leq T_0$  the same set of equations holds whenever incoherent tunneling dominates the dynamics (and intrawell relaxation effects are still negligible). The validity of such an approach implies either strong enough damping, or sufficiently high temperatures.<sup>7,8,21</sup> The equilibrium dynamics of corresponding fluctuations of this two-state dynamics is then also governed by the same exponential decay rate  $\bar{\Gamma}$ , yielding for the unperturbed ( $A=0$ ) equilibrium power spectrum  $S_N^{(0)}(\omega)$  at the driving frequency  $\omega = \Omega$  the approximation

$$S_N^{(0)}(\Omega) = 4x_0^2(k^+k^-/\bar{\Gamma}^2) \frac{2\bar{\Gamma}}{\bar{\Gamma}^2 + \Omega^2}. \quad (68)$$

Correspondingly, in the limit  $\hbar\beta\Omega \ll 1$ , the (classical or quantum) linear susceptibility  $\tilde{\chi}(\Omega)$  exhibits a quasi-elastic Lorentzian peak of amplitude  $b(T) = 4(x_0^2/k_B T)k^+k^-/\bar{\Gamma}^2$  and width  $\bar{\Gamma}$ . It thus reads

$$\tilde{\chi}(\Omega) = b(T) \frac{1}{1 - i\Omega\bar{\Gamma}^{-1}} + O(\hbar\beta\Omega)^2. \quad (69)$$

In conclusion, whenever the backward and forward quantum escape rates are related by the detailed balance condition  $k^- = k^+ \exp(-\epsilon/k_B T)$  [cf. (50) and Ref. 7], we obtain for the scaled power amplitude  $\tilde{\eta}_1$  the result

$$\tilde{\eta}_1(\Omega) = \pi \left( \frac{V_b}{k_B T} \right)^2 \frac{1}{\cosh^4(\epsilon/2k_B T)} \frac{\bar{\Gamma}^2}{\Omega^2 + \bar{\Gamma}^2}. \quad (70)$$

Likewise, consistent with the condition  $\hbar\beta\Omega \ll 1$ , the cotangent hyperbolicus in (64) can be approximated as the inverse of its argument, and the scaled signal-to-noise-ratio  $\tilde{\mathcal{R}}$  becomes effectively independent of the external frequency  $\Omega$ :

$$\tilde{\mathcal{R}} = \frac{\pi}{2} \left( \frac{V_b}{k_B T} \right)^2 \frac{\bar{\Gamma}/\omega_b}{\cosh^2(\epsilon/2k_B T)}. \quad (71)$$

These two relations in (70) and (71) are the main results of our semiclassical QSR analysis. The basic assumptions

under which they are valid are weak noise (52), small amplitude  $A$ ,  $\hbar\beta\Omega \ll 1$ , and  $T/T_0$  not too small. Several results now follow immediately:

(i) Within a *two-state description* of the incoherent (undriven) dynamics, the linear response theory developed in this section effectively reduces the study of QSR to the computation of two corresponding (semiclassical) quantum escape rates  $k_{\text{qm}}^\pm$  at thermal equilibrium [cf. (67)]. For temperatures sufficiently beyond  $T_0$  we can use Eq. (28) with the approximation  $\Lambda_1^b = \lambda_1^b$ , as discussed below (32), to obtain

$$\bar{\Gamma} = f_{\text{qm}} \frac{\mu_b^+ \omega_0}{2\pi\omega_b} \exp\{-\beta V_b\} 2 \cosh(\beta\epsilon/2), \quad (72)$$

$$f_{\text{qm}} = \prod_{n=1}^{\infty} \frac{+\omega_0^2 + n^2\nu^2 + n\nu\gamma}{-\omega_b^2 + n^2\nu^2 + n\nu\gamma} = \frac{\Gamma(1 - \mu_b^+/\nu)\Gamma(1 - \mu_b^-/\nu)}{\Gamma(1 - \mu_0^+/\nu)\Gamma(1 - \mu_0^-/\nu)}. \quad (73)$$

Here, we have exploited (18), (50), and (51) and we have introduced the notations

$$\nu = 2\pi/\hbar\beta, \quad (74)$$

$$\gamma = \eta/m, \quad (75)$$

$$\alpha = \gamma/2\omega_b, \quad (76)$$

$$\mu_b^\pm = \omega_b[\alpha \pm (\alpha^2 + 1)^{1/2}], \quad (77)$$

$$\mu_0^\pm = \omega_b[\alpha \pm (\alpha^2 - (\omega_0/\omega_b)^2)^{1/2}]. \quad (78)$$

Further,  $\Gamma(\dots)$  in (73) denotes the gamma function. Identifying  $\mu_b^+$  with  $\mu$  from (19), the crossover temperature (27) takes the form

$$T_0 = \mu_b^+ \hbar/2\pi k_B. \quad (79)$$

Explicit results for the scaled signal-to-noise ratio  $\tilde{\mathcal{R}}$  are depicted in Fig. 6, and the scaled amplification for QSR is shown with Fig. 7. We note that quantum tunneling can enhance the classical result by almost two orders of magnitude!

(ii) By construction, a linear response approximation does hold independent of whether the coherent applied signal (49) involves adiabatic or nonadiabatic frequencies  $\Omega$ . Hence, Eqs. (63) and (64) hold for *any* driving frequency  $\Omega$ . On the other hand, while the expression (69) for the linear susceptibility  $\tilde{\chi}(\Omega)$  becomes *exact* in the classical limit, the condition  $\hbar\beta\Omega \ll 1$  requires some care in the semiclassical and deep quantum regimes, and may lead to restrictions on the values of the applied driving frequency  $\Omega$ : Whenever the condition  $\hbar\beta\Omega \ll 1$  is not fulfilled, the linear susceptibility  $\tilde{\chi}(\Omega)$  (and hence  $\tilde{\eta}_1$  and  $\tilde{\mathcal{R}}$ ) exhibits a more complicated dependence on the frequency  $\Omega$ , as determined by the full quantum fluctuation dissipation theorem (61) and by the Kramers–Kronig relationships between its real and imaginary parts (see also the next section for a discussion of QSR in the deep quantum regime).

(iii) Because Eqs. (70) and (71) hold independent of whether the escape mechanism is classical or quantum, some general features of QSR can be stated. For the case of weak

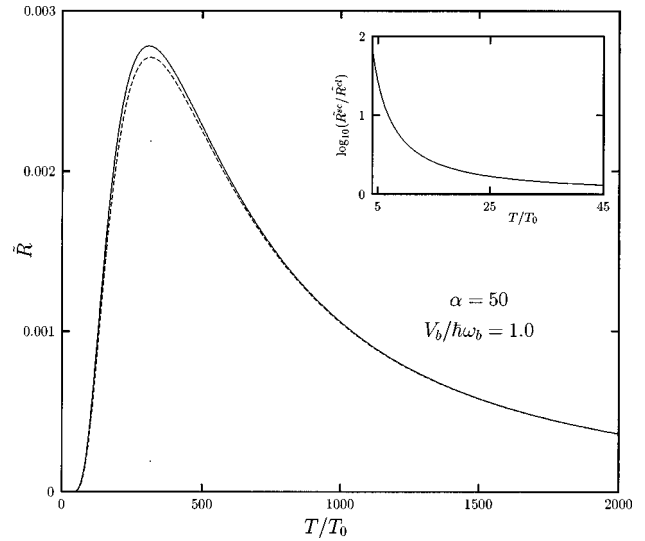


FIG. 6. Quantum stochastic resonance according to (71)–(79) at zero asymmetry ( $\epsilon=0$ ) versus dimensionless temperature  $T/T_0$ , with  $T_0$  the crossover temperature to tunneling dominated escape, as characterized by the semiclassical scaled signal-to-noise ratio  $\tilde{\mathcal{R}}^{\text{sc}}$  (solid line). For comparison the *classical* signal-to-noise ratio is also depicted (dashed line), obtained by setting  $f_{\text{qm}}=1$  in (72). The inset makes clear that the enhancement of the semiclassical  $\tilde{\mathcal{R}}^{\text{sc}}$ , over the corresponding classical signal-to-noise ratio  $\tilde{\mathcal{R}}^{\text{cl}}$ , can reach almost two orders of magnitude.

external signals considered in Eqs. (70) and (71), both the scaled spectral amplification  $\tilde{\eta}_1$  and the scaled signal-to-noise ratio  $\tilde{\mathcal{R}}$  are independent of the external strength  $A$ , but only  $\tilde{\eta}_1$  is still a function of the external frequency  $\Omega$ . Hence, the position  $T_{\mathcal{R}}^*$  of the temperature maximum of the

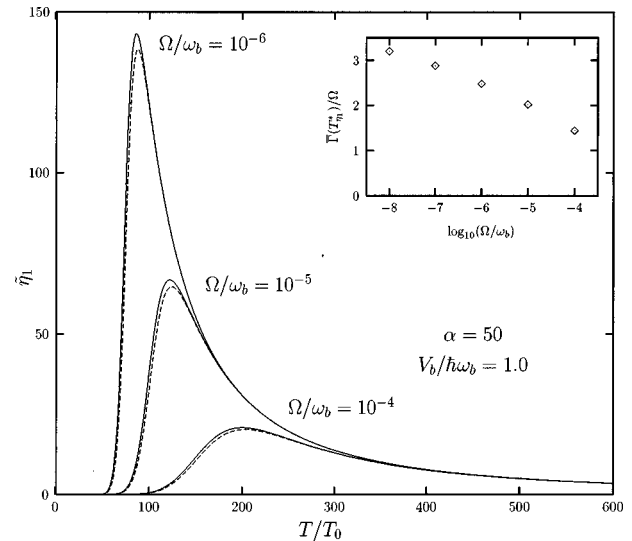


FIG. 7. Scaled spectral amplification  $\tilde{\eta}_1$  [see (70)] versus dimensionless temperature for different driving frequencies  $\Omega$  (solid lines). For comparison, the dashed lines give the results for the classical stochastic resonance spectral amplification (see also Fig. 6). The inset depicts the ratio between the total (forward plus backward) quantum rate  $\bar{\Gamma}$  and  $\Omega$  at the temperature  $T_{\mathcal{R}}^*$  where  $\tilde{\eta}_1$  assumes its maximum. The QSR maximum is thus (at low driving frequencies) only roughly determined by the condition that twice the escape time, i.e.,  $4[\bar{\Gamma}(T_{\mathcal{R}}^*)]^{-1}$ , should approximately be equal to the external driving period  $2\pi/\Omega$  (see Ref. 6).

scaled SNR effectively depends only on *intrinsic* parameters of the bistable system, such as the barrier height  $V_b$ , the asymmetry  $\epsilon$ , the relaxational angular frequencies  $\omega_b$  and  $\omega_0$ , and the friction coefficient  $\eta = m\gamma$ . On the other hand, QSR for  $\tilde{\eta}_1$  can be *externally controlled* by varying the applied driving frequency  $\Omega$ .

(iv) On the same basis as in (iii), the generality of Eqs. (70) and (71) implies that the differences between classical, semiclassical or quantum SR are determined *solely* by the explicit temperature dependence of the escape rates  $k^\pm$ . In particular, the classical [cf. (18)] and the semiclassical escape rates [cf. (73)] decay exponentially as the temperature decreases. This, together with the (classical and semiclassical) condition (52), necessary for a clear-cut separation of time scales, implies that the QSR maxima are determined by the competition between this exponential decay and the algebraic divergence  $(k_B T)^{-2}$  in  $\tilde{\eta}_1$  or in  $\tilde{\mathcal{R}}$  as the temperature is decreased. Hence, the detailed balance factor  $\cosh^{-2}(\epsilon/2k_B T) \ll 1$  only plays a minor role; it always suppresses the SR phenomenon: With  $\exp(-\epsilon/k_B T) \ll 1$ , i.e.,  $\bar{\Gamma} \approx k_{\text{qm}}^+$ , the power amplification  $\tilde{\eta}_1$  is exponentially reduced proportional to  $[\exp(-\epsilon/k_B T)]^2$ ; likewise, the SNR is exponentially (but weaker) reduced proportional to  $\exp(-\epsilon/k_B T)$ . This finding is in accordance with prior studies of classical SR in nonequilibrium systems.<sup>6</sup>

#### D. Quantum stochastic resonance at very low temperatures

Let us comment here in some detail on the situation in the deep cold at extreme low temperatures. As we have seen above, the main challenge in QSR consists in the evaluation of corresponding quantum expectation and correlation functions in a driven, dissipative metastable quantum system. This task, as we have witnessed with the quantum ratchet problem, up to these days has not been possible to solve by analytical means in the whole temperature regime. This objective has never been solved either for the much simpler situation of its classical limit. A useful analytical scheme is possible, however, in the deep quantum regime. In this latter regime the physics is mainly ruled by the dissipative, driven dynamics of the *two lowest tunneling split levels*. This typifies the so-termed dissipative spin-boson problem which has been studied in the *absence* of external driving thoroughly over the last two decades or so, with four authoritative reviews being available.<sup>8</sup> Only in recent years, however, has this problem been addressed in the presence of driving. A few relevant works are listed in Ref. 22. Most importantly, the quantum rates no longer exhibit an exponential Arrhenius-type behavior. Instead, the exponential quantum rate assumes a much smoother (non-Arrhenius-like) temperature dependence and remain finite even at zero temperature.<sup>7,8</sup> Further, within a two-level description of the incoherent tunneling dynamics, the energy splitting of the two discrete energy levels is of the order of the asymmetry energy  $\epsilon$ . Hence, the detailed balance factor represents the relative occupation of the energy levels and it is this factor that starts to play a crucial role for QSR in the deep cold. Now, when  $\epsilon \ll k_B T$ , the energy levels become almost

equally occupied, so that the limit  $\epsilon=0$  yields (with  $\alpha < 1$ ) no QSR phenomenon.<sup>20,23</sup> As a result, in the limit of zero asymmetry  $\epsilon=0$  generally *no* QSR does occur.

Moreover, at such low temperatures the driven quantum dynamics is generally no longer incoherent; i.e., rate descriptions of the type in (66) are not valid. In this regime *incoherent* and *coherent* tunneling events, with the latter occurring predominantly at weak dissipation, low temperatures and/or at nonadiabatic driving frequencies  $\Omega$ . In the last three years, much progress has been made in investigating QSR in this regime. We refer the readers to a recent review of the behavior of nonlinear QSR in the driven spin boson model. See Sec. VI A in Ref. 6, or go directly to the relevant original literature: (i) Within linear response and adiabatic driving, incoherent QSR has been studied by Löfstedt and Coppersmith in Ref. 23, (ii) analytical ‘‘linear’’ and nonlinear QSR, both within coherent and incoherent tunneling regimes at adiabatic and nonadiabatic driving  $\Omega$ , has been investigated by Grifoni and Hänggi.<sup>20</sup> New features, such as driving-induced resonances and quantum coherences, occur in the nonadiabatic driving regime. Moreover, nonlinear QSR also exhibits for its amplification of higher harmonics novel phenomena such as multiple quantum noise-induced suppressions of superharmonic power amplitudes together with typical phase-shift discontinuities.

Insightful exact numerical path integral studies for a driven, dissipative spin-boson model have recently been carried out by Makri.<sup>24</sup> The extension of this numerical approach into the regime mediating between such dissipative two-level models and the semiclassical limit has been worked out in Ref. 25, revealing a multitude of new interesting aspects of QSR.

As a general feature of nonlinear QSR one finds that a principal maximum in the response versus temperature appears when the static asymmetry exceeds the driving frequency *and* driving strength. Moreover, nonlinear QSR exhibits a quantum fluctuation-induced *suppression* of higher harmonics, together with a characteristic phase shift.<sup>20</sup>

#### IV. CONCLUSIONS

In summary, we have investigated the constructive role of quantum fluctuations for noise-driven transport in rocked quantum ratchets and for the phenomenon of stochastic resonance in periodically driven bistable quantum systems. The underlying quantum dynamics in both cases is dissipative, but not necessarily overdamped. As such we have accounted for fluctuation-driven transport in the presence of finite inertia effects (finite mass  $m$ ).<sup>26</sup> We have found that quantum noise can substantially *enhance*, but sometimes also *suppress*, the nonlinear response due to the external periodic driving.

While several ingredients, such as the coupling to a thermal heat bath and the driving out of equilibrium by an external force, as well as the general technical framework, are the same for both our model of a quantum Brownian motor and QSR, the basic mechanisms and the typical observables are different. In the first case, the salient point is the simultaneous breaking of the spatial symmetry and of the detailed

balance symmetry (thermal equilibrium), while in the second case it is the presence of some kind of threshold.

The phenomena of QSR and quantum ratchets in the presence of quantum tunneling carries a great potential for applications. The new effects may be detected experimentally by measuring the ac-quantum transport in mesoscopic metals, in ac-driven atomic force microscopy or via quantum noise-induced currents in periodically forced periodic quantum structures such as semiconductor superlattices or in optical lattices formed by interfering light waves.<sup>27</sup> Yet another class is provided by noise-driven macroscopic quantum systems, such as a properly designed superconducting interference device composed of Josephson junctions. For the latter class, a characteristic rectification effect due to the ratchet effect has been realized and studied in the classical limit already in Ref. 28. Hence, like in the case of classical noise, pure quantum noise does not represent a nuisance but rather can be a useful tool when it interacts with external periodic perturbations.

We remark that in all our explicit examples (Figs. 2–4, 6, and 7) we worked with dimensionless quantities, thus covering microscopic, mesoscopic, and even macroscopic potential applications as mentioned above. The (dimensionless) corrections of purely classical predictions due to quantum effects may be summarized as follows: Even above the tunneling-dominated temperature regime the particle current may be enhanced up to a factor of 10 in a quantum ratchet, and as the temperature is further decreased, this correction factor increases up to infinity! Even more, when correctly including quantum effects, the sign of the current may become opposite to that of the classical prediction. Finally, lowering the temperature to zero does not bring the ratchet current to a standstill—as would be expected classically—but rather it saturates at a finite value. Similarly, in the case of QSR, we have demonstrated enhancement of classical SR up to two orders of magnitude due to quantum tunneling corrections.

We conclude with a few words about the issue of efficiencies in a quantum ratchet device. While classically this subject has already been addressed from different points of view,<sup>29</sup> for quantum systems matters are apparently more subtle and so far largely unsettled. One may speculate that the quantum efficiency should exceed the classical one because the current is typically increased, and the total consumption of energy should be generally hindered by quantum effects. A more detailed quantitative study of these questions remains as an interesting topic for future investigations.

## ACKNOWLEDGMENTS

We thank M. Grifoni and L. Hartmann for fruitful collaborations on the topics of this article and for providing Figs. 5–7. Support of this work by the Deutsche Forschungsgemeinschaft (HA1517/14-2, HA1517/13-2) is gratefully acknowledged.

<sup>1</sup>M. von Smoluchowski, *Phys. Z.* **XIII**, 1069 (1912); see also in R. P. Feynman, R. B. Leighton, and M. Sands, *The Feynman Lectures on Physics* (Addison-Wesley, Reading, MA, 1966), Vol. I, Chap. 46; J. M. R.

Parrondo and P. Espanol, *Am. J. Phys.* **64**, 1125 (1996).

<sup>2</sup>A. Ajdari and J. Prost, *C. R. Acad. Sci. Paris II* **315**, 1635 (1992); M. O. Magnasco, *Phys. Rev. Lett.* **71**, 1477 (1993); R. D. Astumian and M. Bier, *ibid.* **72**, 1766 (1994); C. R. Doering, W. Horsthemke, and J. Riordan, *ibid.* **72**, 2984 (1994).

<sup>3</sup>For reviews see P. Hänggi and R. Bartussek, *Springer-Series Lecture Notes in Physics*, edited by J. Parisi *et al.* (Springer, Berlin, 1996), Vol. 476, pp. 294–308; R. D. Astumian, *Science* **276**, 917 (1997); F. Jülicher, A. Ajdari, and J. Prost, *Rev. Mod. Phys.* **69**, 1269 (1997).

<sup>4</sup>R. Benzi, A. Sutera, and A. Vulpiani, *J. Phys. A* **14**, L453 (1981); C. Nicolis and G. Nicolis, *Tellus* **33**, 225 (1981).

<sup>5</sup>P. Jung, *Phys. Rep.* **234**, 175 (1993); F. Moss, D. Pierson, and D. O’Gorman, *Int. J. Bifurcation Chaos Appl. Sci. Eng.* **4**, 1383 (1994).

<sup>6</sup>L. Gammaitoni, P. Hänggi, P. Jung, and F. Marchesoni, *Rev. Mod. Phys.* **70**, 223 (1998).

<sup>7</sup>P. Hänggi, P. Talkner, and M. Borkovec, *Rev. Mod. Phys.* **62**, 251 (1990).

<sup>8</sup>A. J. Leggett, S. Chakravarty, A. T. Dorsey, M. P. A. Fisher, A. Garg, and W. Zwerger, *Rev. Mod. Phys.* **59**, 1 (1987); *ibid.* **67**, 725 (1995) (erratum); H. Grabert, P. Schramm, and G. L. Ingold, *Phys. Rep.* **168**, 115 (1988); U. Weiss, *Quantum Dissipative Systems*, Series in Modern Condensed Matter Physics, Vol. 2 (World Scientific, Singapore, 1993); A. Benderskii, D. E. Makarov, and C. A. Wight, *Adv. Chem. Phys.* **88**, 1 (1994).

<sup>9</sup>P. Hänggi and W. Hontscha, *J. Chem. Phys.* **88**, 4094 (1988); E. Freidkin, P. S. Riseborough, and P. Hänggi, *Z. Phys. B* **64**, 237 (1986); **67**, 271 (1987) (erratum).

<sup>10</sup>H. Grabert, P. Olschowski, and U. Weiss, *Phys. Rev. B* **36**, 1931 (1987).

<sup>11</sup>A. I. Larkin and Yu. N. Ovchinnikov, *Sov. Phys. JETP* **59**, 420 (1984); H. Grabert and U. Weiss, *Phys. Rev. Lett.* **53**, 1787 (1984); P. S. Riseborough, P. Hänggi, and E. Freidkin, *Phys. Rev. A* **32**, 489 (1985).

<sup>12</sup>S. A. Gurvitz, *Phys. Rev. A* **38**, 1747 (1988) and further references therein.

<sup>13</sup>P. Reimann, M. Grifoni, and P. Hänggi, *Phys. Rev. Lett.* **79**, 10 (1997).

<sup>14</sup>L. D. Chang and S. Chakravarty, *Phys. Rev. B* **29**, 130 (1984); *ibid.* **30**, 1566 (1984) (erratum).

<sup>15</sup>R. Bartussek, P. Hänggi, and J. G. Kissner, *Europhys. Lett.* **28**, 459 (1994).

<sup>16</sup>P. Reimann, *Phys. Rep.* **290**, 149 (1997).

<sup>17</sup>M. Grifoni, L. Hartmann, S. Berchtold, and P. Hänggi, *Phys. Rev. E* **53**, 5890 (1996); *ibid.* **56**, 6213 (1997) (erratum).

<sup>18</sup>P. Jung and P. Hänggi, *Europhys. Lett.* **8**, 505 (1989); *Phys. Rev. A* **44**, 8032 (1991).

<sup>19</sup>B. McNamara and K. Wiesenfeld, *Phys. Rev. A* **39**, 4854 (1989).

<sup>20</sup>M. Grifoni and P. Hänggi, *Phys. Rev. Lett.* **76**, 1611 (1996); *Phys. Rev. E* **54**, 1390 (1996).

<sup>21</sup>U. Weiss, H. Grabert, P. Hänggi, and P. Riseborough, *Phys. Rev. B* **35**, 9535 (1987).

<sup>22</sup>M. Grifoni, M. Sassetti, J. Stockburger, and U. Weiss, *Phys. Rev. E* **48**, 3497 (1993); T. Dittrich, B. Oelschlägel, and P. Hänggi, *Europhys. Lett.* **22**, 5 (1993); *Acta Phys. Pol. B* **94**, 845 (1993); Y. Dakhnovskii, *Phys. Rev. B* **49**, 4649 (1994); *Ann. Phys.* **230**, 145 (1994); I. A. Goychuk, E. G. Petrov, and V. May, *Phys. Rev. E* **52**, 2392 (1995); *Chem. Phys. Lett.* **353**, 428 (1996); M. Grifoni, M. Sassetti, P. Hänggi, and U. Weiss, *Phys. Rev. E* **52**, 3596 (1995); M. Grifoni, M. Sassetti, and U. Weiss, *Phys. Rev. E* **53**, R2033 (1996).

<sup>23</sup>R. Löfstedt and S. N. Coppersmith, *Phys. Rev. Lett.* **72**, 1947 (1994); *Phys. Rev. E* **49**, 4821 (1994).

<sup>24</sup>N. Makri, *J. Chem. Phys.* **106**, 2286 (1997).

<sup>25</sup>M. Thorwart and P. Jung, *Phys. Rev. Lett.* **78**, 2503 (1997); M. Thorwart, P. Reimann, P. Jung, and R. F. Fox, *Phys. Lett. A* **239**, 233 (1998).

<sup>26</sup>P. Jung, J. G. Kissner, and P. Hänggi, *Phys. Rev. Lett.* **76**, 3436 (1996); B. Lindner, L. Schimansky-Geier, P. Reimann, and P. Hänggi, in *Applied Nonlinear Dynamics and Stochastic Systems near the Millennium*, edited by J. B. Kadtko and A. Bulsara, *AIP Conf. Proc.* **411**, 309 (1997).

<sup>27</sup>V. S. Letokhov, V. G. Minogin, and B. D. Pavlik, *Zh. Eksp. Teor. Fiz.* **72**, 1328 (1974); A. Hemmerich and T. W. Hänsch, *Phys. Rev. Lett.* **70**, 410 (1993); G. Grynberg, B. Lounis, P. Verkerk, J.-Y. Courtois, and C. Salomon, *Phys. Rev. Lett.* **70**, 2249 (1993); S. R. Wilkinson, C. F.

- Bharucha, K. W. Madison, Qian Niu, and M. G. Raizen, *Phys. Rev. Lett.* **76**, 4512 (1996); M. G. Prentiss, *Science* **260**, 1078 (1993).
- <sup>28</sup>I. Zapata, R. Bartussek, F. Sols, and P. Hänggi, *Phys. Rev. Lett.* **77**, 2292 (1996); I. Zapata, J. Luzcka, F. Sols, and P. Hänggi, *Phys. Rev. Lett.* **80**, 829 (1998).
- <sup>29</sup>R. D. Vale and F. Oosawa, *Adv. Biophys.* **26**, 97 (1990); M. Bier and R. D. Astumian, *Bioelectrochemistry and Bioenergetics* **39**, 67 (1996); K. Sekimoto, *J. Phys. Soc. Jpn.* **66**, 1234 (1997).